

MICROSCALE NUMERICAL SIMULATION OF YARN TENSILE BEHAVIOR USING A HIGH-FIDELITY GEOMETRICAL FIBER MODEL EXTRACTED FROM MICRO-CT IMAGING

AXEL BRAL¹, LODE DAELEMANS² AND JORIS DEGROOTE^{1,3}

¹Department of Electromechanical, Systems and Metal Engineering
Ghent University
Sint-Pietersnieuwstraat 41, 9000 Ghent, Belgium
e-mail: Axel.Bral@UGent.be, www.fsi.ugent.be

²Department of Materials, Textiles and Chemical Engineering (MaTCh)
Ghent University
Technologiepark 46/70, 9052 Zwijnaarde, Belgium

³Flanders Make
Ghent, Belgium

Key words: Fiber Model, Finite element analysis, Microcomputed Tomography, Tensile Test, Yarn

Abstract. Air jet weaving, where the weft yarn is transported through the machine using air as propelling medium, is a popular weaving method due to its superior productivity, however at the cost of a high energy demand. The interactions between the weft yarn and the air jets are complex and not yet fully understood. Moreover, state-of-the-art techniques to simulate these interactions, are far from mature since the yarn is often simplified as a smooth and solid cylinder. Therefore, a novel multi-scale and multi-physics approach is proposed to simulate the interaction between weft yarns and air jets. Starting from microcomputed tomography (μ CT) scans of a yarn used in air jet weaving, a high-fidelity microscale geometrical model is constructed, representing the yarn by its fibers. This geometrical model is used as input for microstructural simulations and will be used for flow simulations on microscale, where the aim is to extract local coefficients and as such characterize the yarn. These coefficients are then used as input for computationally cheap macroscale models, where the yarn is represented by its centerline containing the microscale properties. In a final stage, the macroscale structural and flow models will be coupled as to obtain a full FSI simulation of a weft insertion in an air jet loom. Current paper highlights the microscale geometry extraction of a fine wool fiber yarn of 28.8 tex. Consecutively, a computational framework is proposed to simulate the tensile behavior of this yarn, using the previously obtained microscale geometrical model. The resulting stress-strain curve of the yarn is compared to experiments and shows good correspondence.

1 INTRODUCTION

Air jet weaving looms are popular due to their superior production rate (in the order of 2000 insertions per minute) combined with low maintenance costs when compared to rapier or projectile weaving looms. This is caused by the fact that no mechanical parts are employed to propel the weft yarn across the weaving machine. Instead, compressed air propels the yarn. However, this induces a high energy demand, in the order of 10 kWh/kg of woven fabric [1]. Therefore, energy efficient machinery is critical for both economical and ecological reasons.

Initially, only incremental changes of the machines were made based on intuition and testing, contributing only to a limited extent towards a better understanding of the interactions between the air jets and the weft yarn. These interactions are rather complex due to the high-speed and non-uniform nature of the flow and due to the irregularity of the yarn structure. Nowadays, researchers more often resort to numerical simulations to characterize these machines. Especially the flow field in the main nozzle of an air jet weaving loom has been studied extensively by means of Computational Fluid Dynamics (CFD), e.g. by He et al. [2]. The flow field induced by relay nozzles in the reed channel was studied by among others Adamek et al. [3]. Even though optimizing the flow field using numerical simulations might benefit the energy use of these weaving machines, it provides no information on the interaction between the flow and the yarns. However, it is precisely this interaction that determines the stability of the weaving process and thus the number of weaving defects.

When studying the air-yarn interaction, one ends up in the domain of Fluid-Structure Interaction (FSI). State-of-the-art FSI simulations of a (partial) weft yarn insertion typically represent the yarn as a smooth and solid cylinder, for example in Delcour et al. [4]. However in reality, most yarns used in air jet weaving consist of tens to hundreds of individual fibers, resulting in an irregular surface appearance, see Figure 1. Therefore, current research develops a numerical workflow to simulate the air-yarn interaction considering the fibrous nature of the yarn.

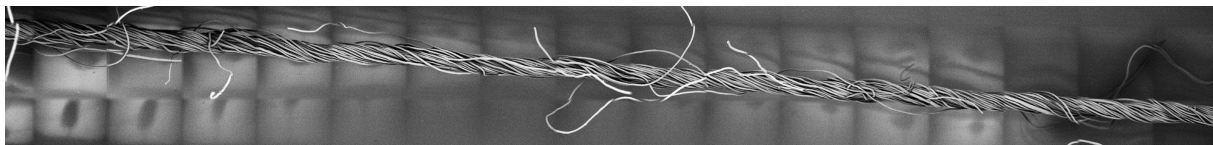


Figure 1: Scanning Electron Microscopy (SEM) image of the surface appearance of a fine wool fiber yarn used in air jet weaving.

Since the fiber diameter is in the order of μm , while the weaving machines have dimensions in the order of meters, simulating a complete yarn insertion using a detailed yarn geometry is computationally unfeasible for the foreseeable future. Therefore, a multi-scale and multi-physics approach is adopted, as outlined in Figure 2. In a first stage, a geometrical micromodel of a yarn segment is constructed based on microcomputed tomography (μCT) imaging. This in turn serves as input for both structural and flow simulations. The structural simulations on micro level aim to compute the stiffness (in tension and bending) and yarn-wall friction coefficients which are consecutively used in a structural macromodel that relies on beam theory. This macromodel is computationally light since the yarn properties are considered along a curve (1D space) only. The geometrical and microstructural models are the focus of this work. In future

work, flow simulations on microscale level will be employed to extract local force coefficients that relate the fluid force on the yarn to the flow velocity and direction and will serve as input for an actuator line method [5] on macroscale level. The advantage of this actuator line method is that the yarn geometry is not explicitly considered in the macroscale simulations. Indeed, the forces that the yarn exerts on the flow are smeared out in the flow domain, allowing for a coarser mesh thus reducing the computational cost. Moreover, this actuator line method is in fact a 1D representation of the yarn and as such is compatible with the beam elements on the structural side. In a final stage, these macromodels will be coupled in an FSI simulation of a yarn insertion in an air jet weaving loom.

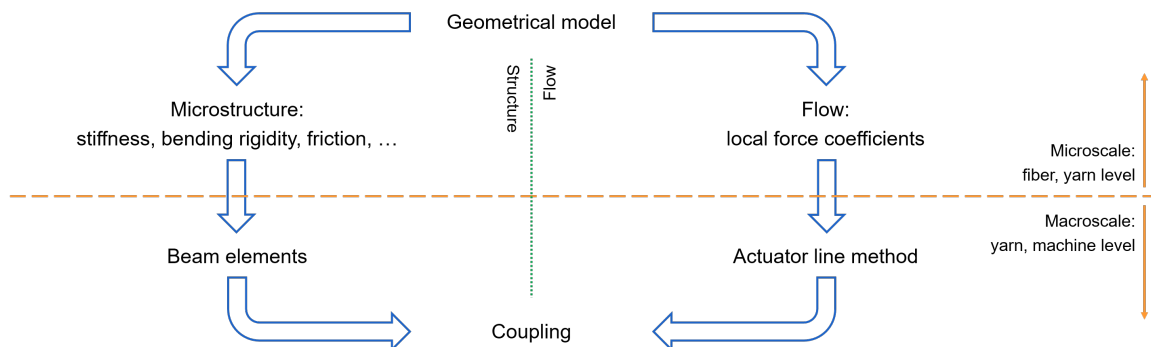


Figure 2: Multi-scale and multi-physics approach to simulate the air-yarn interaction in an air jet weaving machine.

2 METHODOLOGY

Figure 3 shows the main steps followed to characterize a wool fiber yarn’s mechanical behavior on microscale level. The subsequent sections elaborate on each substep.

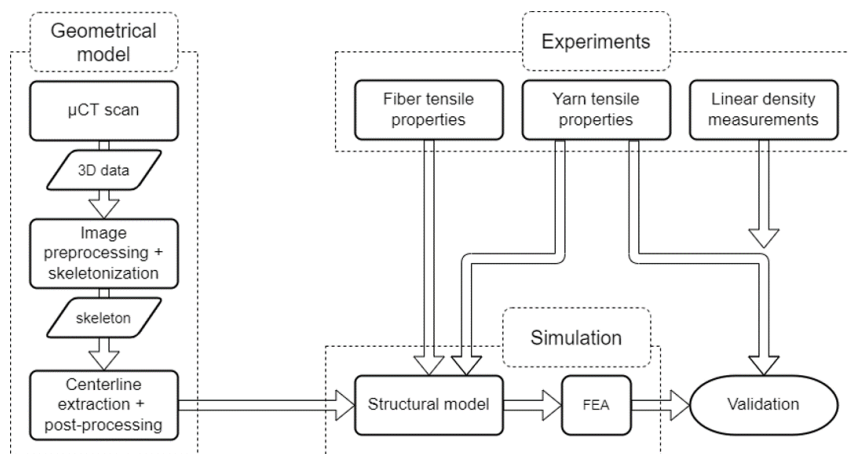


Figure 3: Overview of the methodology to characterize a yarn’s tensile properties using Finite Element Analysis (FEA) based on a high-fidelity geometrical yarn model.

2.1 Geometrical extraction procedure

As shown in Figure 3, the creation of a high-fidelity geometrical fiber model starts from μ CT data. The data consist of 3458 slices of 732 by 919 cubic voxels with an edge length of $1.29852 \mu\text{m}$ leading to a total sample length along the yarn axis of 4.491 mm. A portion of the yarn core in such a slice is shown in Figure 4a. This data set is transferred to a second step in the geometrical model extraction procedure, i.e. the image preprocessing and skeletonization step. To obtain such a skeleton, which contains in fact the centerlines of the fibers, the original slices first need to be binarized (Figure 4b) in order to obtain two discrete phases: fiber material (in white) and background (in black). However, the fibers in these binarized slices are often still erroneously connected. If they were skeletonized straight away, these connections would still exist in the skeleton, which is unwanted behavior. Therefore, in an intermediate step, these connections are broken by searching for saddle points in the Euclidean Distance Transform (EDT) of the original binary slices. The result of this intermediate step is shown in Figure 4c. Subsequently, the modified binaries are stacked and the resulting 3D matrix is skeletonized using the algorithm of Lee et al. [6], see Figure 4d.

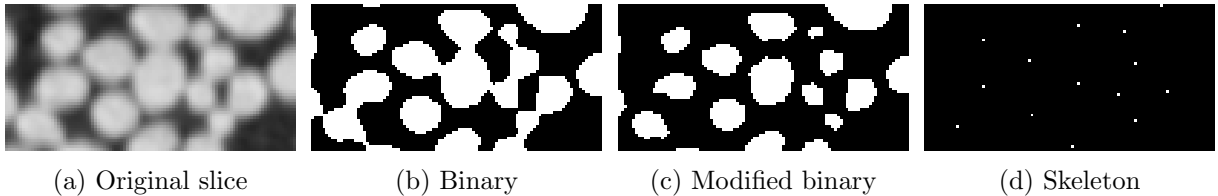


Figure 4: Illustration of the intermediate results obtained in the image preprocessing algorithm.

The skeleton obtained in previous step is a $732 \times 919 \times 3458$ binary matrix containing ones at the location of a fiber centerline and zeros elsewhere. Subsequently, these centerlines are extracted from the matrix using graphs. As such, an ordered list of coordinates is obtained for each fiber centerline. In the final step, these centerlines are post-processed. This step consists of smoothing the centerlines using cubic B-splines, removing outliers (i.e. fiber segments from a second yarn that was scanned together with current sample), aligning the yarn axis with the z-axis, assigning a fiber diameter to the centerlines and avoiding overlap between the fibers. The resulting geometrical micromodel is shown in Figure 5.

2.2 Experimental setup

The experimental part of this paper serves the purpose to firstly provide the necessary inputs to the structural model in terms of material properties and boundary conditions and secondly to provide validation data to compare with the results of the structural simulations.

Firstly, the fiber's tensile properties were determined according to the EN ISO 5079 (2020) norm. Individual fibers with a sample length of 20.0 mm were isolated (100 samples). Subsequently their linear density and tensile behavior were tested using the Textechno Favimat with a load cell of 210 cN. The fiber diameter was inferred from the measured linear density and the volumetric density of wool, 1310 kg/m^3 . These measurements lead to stress-strain relationships for the fibers, as shown in color in Figure 6, and this data was used as input for the structural

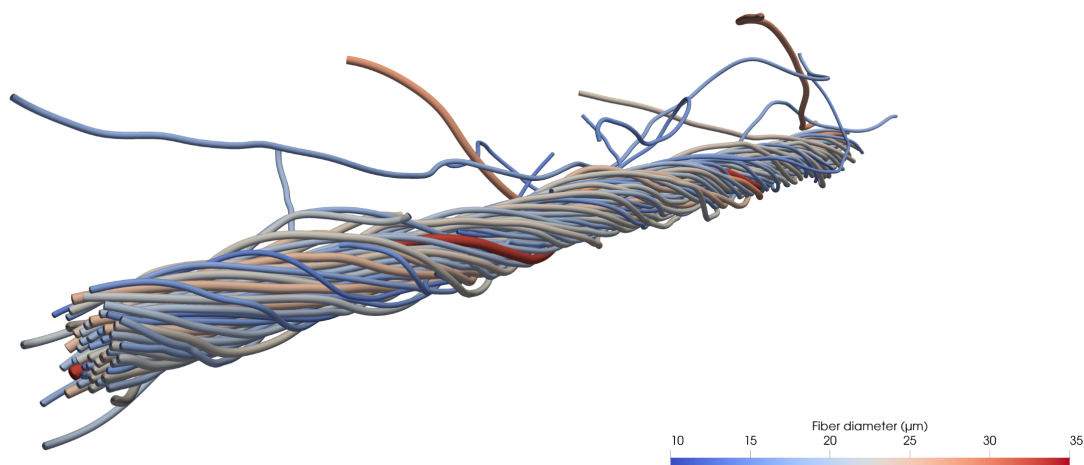


Figure 5: Resulting geometrical micromodel of a fine wool fiber yarn (28.8 tex) extracted from μ CT data.

model in Section 2.3.

Subsequently, the yarn's tensile properties were measured. To achieve this, 50 samples with a gauge length of 500 mm were tested using the Textechno Statimat M with a load cell of 10 N, complying to the EN ISO 2062 (2010) norm. The boundary conditions, i.e. the test speed of 500 mm/min, served as input for the structural model as well. In contrast, the resulting force-elongation relationships were used as validation data for the simulations.

Finally, the yarn's linear density was measured by weighing a sample of 100 m, according to the ISO 2060 (1994) norm. The resulting density, equal to 28.8 tex, was used to convert the force-elongation curves from the Textechno Statimat M to stress-strain relationships for the yarn's tensile properties and to compare to the linear density of the geometrical model (27.4 tex).

2.3 Structural model

A first input to the structural model was the geometrical micromodel derived in Section 2.1, containing the locations and diameters of the fibers. The fibers were discretized in Abaqus 2021 (Dassault Systèmes) using linear Timoshenko beam elements (B31), resulting in a mesh of 13737 elements. The volumetric density of these fibers was set to 1310 kg/m³.

Secondly, the stress-strain relationship of the fibers was derived from the experiments, discussed above in Section 2.2. Figure 6 shows the used material relationship (in black) compared to the experiments. This bilinear behavior corresponds to an initial elastic region of 3.45 GPa followed by a plastic region. The apparent stiffer region of the fibers in the experiments (at elongations > 30 %) was not modeled since these high strains are out of interest for weaving and are consequently not attained in current simulations. The extension towards these higher strains is straightforward, however. Fiber failure was not accounted for in current model. The shear modulus of the fibers was set to 1.5 GPa and the inter-fiber friction coefficient to 0.25.

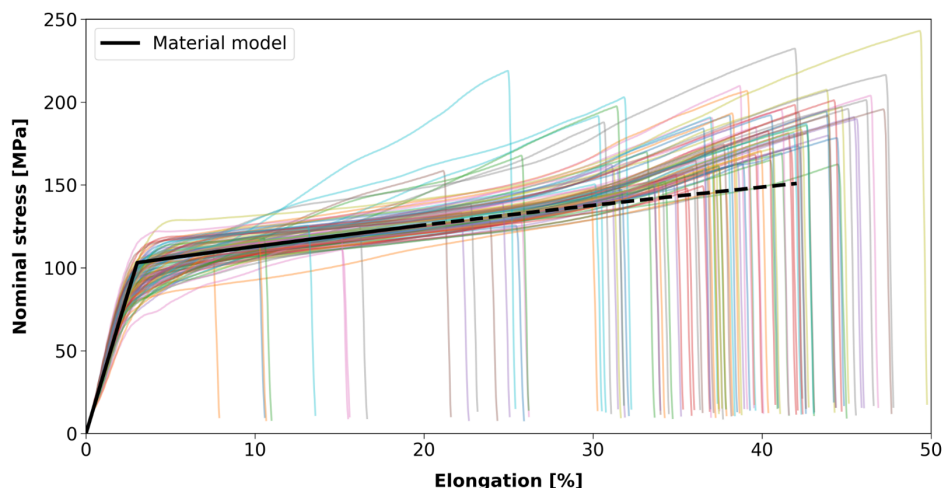


Figure 6: Experimentally measured stress-strain curves of the wool fibers (in color) as input for the modeled fiber behavior (in black). The dashed portion of the black stress-strain curve was not reached in the simulations.

As a final material parameter, Rayleigh damping was enabled to remove oscillations from the resulting stress-strain curve. The mass proportional damping factor was set to 3028 s^{-1} while the stiffness proportional damping factor was disabled due to its adverse impact on the stable time step. To assess the influence of this parameter on the solution, its value was decreased with a factor 10, leading to a similar but more noisy appearance of the stress-strain curve. Alternatively, increasing this parameter with a factor 10 lead to an upwards shifted and distorted stress-strain curve, meaning that unphysical reaction forces were induced in the material.

From the set-up of the yarn tensile test (Section 2.2), the test speed was used as boundary condition. One end was clamped, the other end was given a constant velocity of 500 mm/min. These boundary conditions were applied to two reference points defined at the ends of the yarn and were transmitted to the fibers by means of a kinematic coupling, which constrained all but the radial direction.

For the simulation, the explicit solver of Abaqus 2021 was opted for. The stable timestep size was raised to 10^{-7} s by means of uniform variable mass scaling, allowing for a faster simulation without introducing significant inertial effects. A yarn elongation of 15 % with respect to the initial sample length was aimed for, and therefore the simulation was stopped after 0.081 s.

3 RESULTS AND DISCUSSION

In contrast to purely experimental campaigns or theoretical structural models, where the stress-strain relationships for yarns are derived analytically assuming simplified geometries, current simulation strategy allows to gain insight in the stress distribution along individual fibers inside a yarn with a realistic geometry. Figure 7 shows such axial stress distribution along a staple fiber with free end inside the yarn core. It is clear that the axial stress gradually decreases to zero close to the free fiber end.

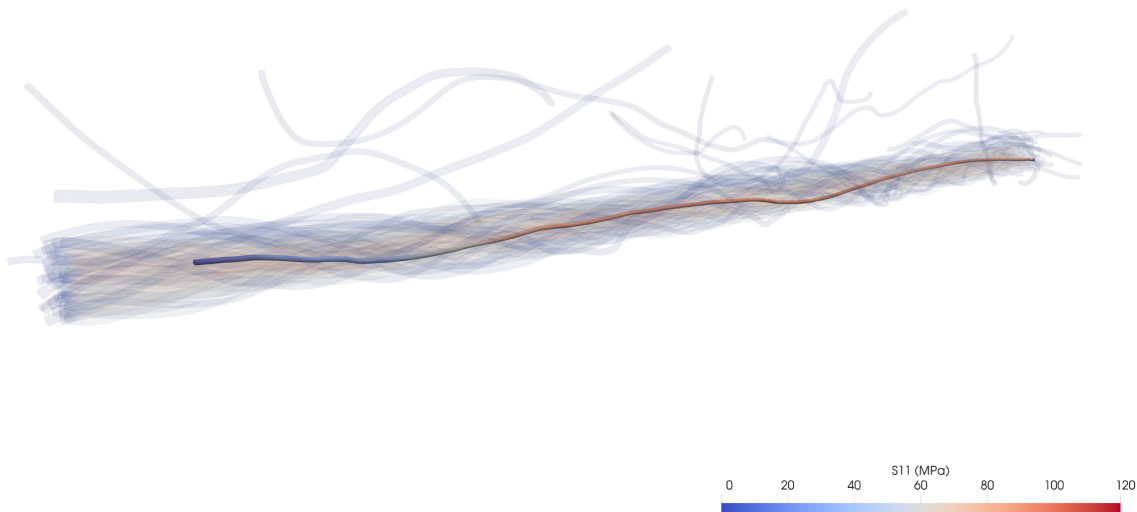


Figure 7: Axial stress distribution along the centerline of a fiber with free end inside the yarn core for a yarn elongation of 2.5 %.

Figure 8 shows the axial stress distribution through a cross section of the yarn. It follows that the stress build-up during a tensile test starts centrally, while the outer fibers reorganize. However, this build-up is not uniform in the center, owing to the irregular and non-ideal geometry that is incorporated in current model. The small fiber overlap is caused by the contact algorithm used in Abaqus. For interactions between structures consisting of beam elements, only a penalty-based contact algorithm is possible. This means that contacting fibers experience a contact pressure that is proportional to the fiber overlap and a penalty stiffness. Therefore, small fiber overlap is unavoidable.

To assess the validity of the proposed simulation strategy, the stress-strain relationship of the simulated yarn is compared to experiments, see also Figure 9. The simulated yarn stress is computed as the reaction force obtained from the moving reference point divided by a virtual yarn cross section inferred from the linear density in the model (27.4 tex) and the volumetric density of wool (1310 kg/m^3). It is clear that even though the material model is simplified, the simulated stress-strain curve fits well in the envelope of the experiments due to the inclusion of the detailed geometry. At large strains ($> 5 \%$), the simulated yarn behavior is slightly stiffer than the experiments. This is believed to be caused by omitting fiber failure in the structural model.

The computational cost for this microscale tensile simulation amounts to 3.5 hours on 20 cores of a 2x20-core Intel Xeon Gold 6242R 3.1GHz machine.

Finally, the simulated yarn behavior under axial load as result of the microscale simulations serves as input for the macroscale yarn model presented in Figure 2. Additionally, the bending behavior and yarn-wall friction on microscale level will be investigated in future work. Note that the obtained microscale geometry (see Figure 5), also serves as input for the microscale flow simulations as to investigate the local force coefficients of the yarn.

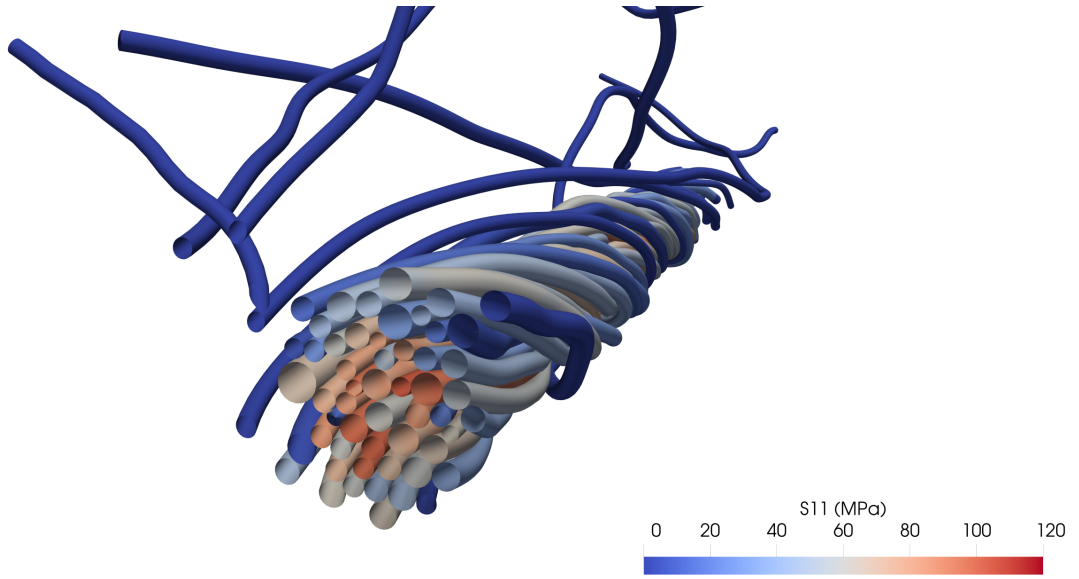


Figure 8: Axial stress distribution in a cross section of 2.45 mm from the origin for a yarn elongation of 2.5 %.

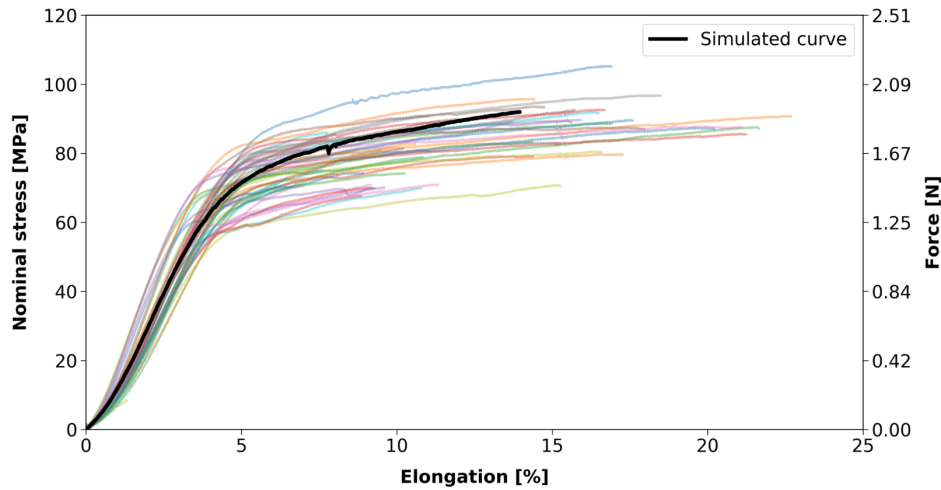


Figure 9: Experimentally measured stress-strain curves of the wool yarn (in color) as validation data for the simulation (in black).

4 CONCLUSION

This paper investigates the tensile behavior of a fine wool fiber yarn (28.8 tex) by means of microstructural simulations in the framework of a multi-physics and multi-scale workflow to simulate the interaction between weft yarns and air jets in an air jet weaving machine. To achieve this, a 3D image of a yarn sample was constructed using microcomputed tomography. Before tracing the individual fibers using a skeletonization algorithm, the slices were preprocessed

such that the fibers are disconnected from each other. Once the individual fiber centerlines were extracted from the skeleton, a postprocessing stage was initiated where these raw centerlines were smoothed, the fiber diameter was set and overlap between the fibers was avoided. The resulting microscale geometrical model was then used as a starting point for the structural simulation of a tensile test. Material properties and boundary conditions followed from the experimental tensile tests on the fibers and yarn, respectively. Abaqus 2021 was employed to perform the structural simulations. The resulting simulated stress-strain curves were compared to the experiments and show excellent agreement. This paper thus shows that the tensile behavior of this yarn can be predicted using a detailed geometrical model and average fiber material properties.

FUNDING

The authors gratefully acknowledge the funding by the Ghent University Special Research Fund (BOF) with project number 01D04520 (01 November 2020 - 31 October 2021) and by the Research Foundation Flanders (FWO) with project number 1S30822N (as from 01 November 2021).

REFERENCES

- [1] Grassi, C., Schröter, A., Gloy, Y., et al. Energy efficiency approach to reduce costs of ownership of air jet weaving. *International Journal of Chemical, Molecular, Nuclear, Materials and Metallurgical Engineering* (2016) **10**(12):1417-1423.
- [2] He, S., Qian, Y., Xue, W., et al. Numerical simulation of flow field in air-jet loom main nozzle. *AUTEX Research Journal* (2019) **19**(2):181-190.
- [3] Adamek, K., Karel, P., Kolar, J., et al. Relay nozzles and weaving reed. *International Journal of Mechanical Engineering and Applications* (2015) **3**(1-1):13-21.
- [4] Delcour, L., Peeters, J. and Degroote, J. Three-dimensional fluid-structure interaction simulations of a yarn subjected to the main nozzle flow of an air-jet weaving loom using a Chimera technique. *Textile Research Journal* (2020) **90**(2):194-212.
- [5] Troldborg, N., Sorensen, J.N. and Mikkelsen, R. Numerical simulations of wake characteristics of a wind turbine in uniform flow. *Wind Energy* (2010) **13**:86-99.
- [6] Lee, T.C., Kashyap, R.L. and Chu, C.N. Building skeleton models via 3-D medial surface axis thinning algorithms. *CVGIP: Graphical Models and Image Processing* (1994) **56**:462-478.